Proceedings of the Fifth Lunar Conference
(Supplement 5, Geochimica et Cosmochimica Acta)
Vol. 3 pp. 2827–2839 (1974)
Printed in the United States of America

Magnetic properties of Apollo 11–17 lunar materials with special reference to effects of meteorite impact

T. NAGATA
National Institute of Polar Research, Japan

N. SUGIURA
Geophysical Institute, University of Tokyo, Japan

R. M. FISHER and F. C. SCHWERER
U.S. Steel Corporation, Research Laboratory, Monroeville, Pennsylvania

M. D. FULLER and J. R. DUNN
Department of Earth and Planetary Sciences, University of Pittsburgh, Pittsburgh, Pennsylvania

Abstract—The magnetic properties of four Apollo 16 samples and six Apollo 17 samples have been studied. Apollo 17 site basaltic rocks have the typical magnetic properties of lunar mare basalts, while an Apollo 17 site anorthositic gabbro magnetically similar to Apollo 16 site anorthositic rocks. Apollo 17 site orange soil contains an unknown ferromagnetic component in addition to almost pure iron, and the particular component changes to iron by heating.

NRM and its stability of four Apollo 16 samples and seven Apollo 17 samples have been examined. Four samples among them have a reasonably stable component of NRM of 10^{-6} emu/g in the order of magnitude.

All Apollo 11–17 lunar materials examined to date more or less contain a ferromagnetic metal component of almost pure iron, and lunar breccias and fines contain ferromagnetic metal about ten times as much as that in lunar basaltic rocks. Magnetization curves obtained during heating and cooling cycles were analyzed to provide detailed information on the abundance of iron–nickel phases as a function of nickel content for several lunar and meteoritic samples. The high abundance of almost pure iron in breccias and fines is most likely to be the product of breakdown of fayalite, ulvöspinel, ilmenite, and others by severe meteoritic impact. The high abundance of kamacite in lunar breccias, on the other hand, may be due to the mixing of meteoritic kamacite into the lunar surface materials.

INTRODUCTION

THE MAGNETIC PROPERTIES and characteristics of the natural remanent magnetization of Apollo 11 through 16 lunar samples of 30 in total number have been examined by the authors (Nagata *et al.*, 1970, 1971, 1972a, 1972b, 1973). The magnetic properties of four more Apollo 16 samples (60016, 61156-11, 61156-12, and 64435) and six Apollo 17 samples (70017-73, 70017-75, 70215-26, 74220, 75083, and 77017) have recently been studied, and four more Apollo 17 samples (73275, 74275, 78155, and 78500) are under studies at present. According to the preliminary discriptions given in Lunar Sample Information Catalogs Apollo 16 (NASA,

1972) and Apollo 17 (NASA, 1973), the petrographic characteristics of these lunar samples are as follows:

60016: An anorthositic breccia (FeO: 4.28%, Al_2O_3: 28.2%, Ni: 330 ppm),
61156: An annealed blocky breccia (FeO: 7.75%, Al_2O_3: 22.94%, Ni: 184 ppm),
64435: An anorthositic blocky subangular breccia (FeO: 3.13%, Al_2O_3: 30.8%, Ni: 56 ppm),
70017: A blocky subangular coarse basalt (FeO: 18.7%, Al_2O_3: 8.78%),
70215: A fine-grained basalt (FeO: 19.96%, Al_2O_3: 8.86%),
74220: Orange soils (FeO: 22.04%, Al_2O_3: 6.32%, Ni: 83 ppm),
75083: Dark-gray coarse soils,
77017: A crushed anorthositic gabbro (C(FeO) = 6.19%), (FeO: 6.19%, Al_2O_3: 26.59%, Ni: 95 ppm),
73275: A blocky, subangular metaclastic rock, (FeO: 9.05%, Al_2O_3: 18.49%),
74275: A slabby subangular basalt, (FeO: 18.25%, Al_2O_3: 8.51%),
78155: An anorthositic cataclasite (FeO: 5.82%, Al_2O_3: 25.94%, Ni: 53 ppm)
78500: Medium brownish gray soils.

All Apollo 16 samples listed above are anorthositic, while Apollo 17 samples include typical lunar mare basalts (e.g. 70215 and 74275) as well as anorthositic rocks (e.g. 77017 and 78155).

In the present work, the basic magnetic properties of these samples will be summarized and then characteristics of their natural remanent magnetization will be discussed. Including the newly obtained data, the basic magnetic properties of all Apollo 11–17 lunar materials measured by the authors to date will be summarized with a special reference with possible effects of meteorite impact upon the magnetic properties of lunar surface materials.

Basic Magnetic Properties of Apollo 16 and 17 Lunar Materials

In Table 1, the intrinsic and structure-sensitive magnetic parameters of the newly examined Apollo 16 and 17 lunar materials are summarized. The intrinsic magnetic properties are the saturation magnetization (I_s) and the paramagnetic susceptibility (χ_a) measured at 295°K and 4.2°K, and Curie point (Θ) and the $\alpha-\gamma$ transition temperature of FeNi alloy (Θ^*). The structure-sensitive parameters are the saturation remanent magnetization (I_R) and the coercive force (H_c) measured at 295°K and 4.2°K and the initial magnetic susceptibility (χ_0) and the remanence coercive force (H_{RC}) measured at room temperature (295°K).

In general, the magnetic properties of the newly examined Apollo 16 samples are very similar to those of the eight previously studied Apollo 16 samples (Nagata *et al.*, 1973). Namely, (a) their paramagnetic susceptibility (χ_a) is very small proportionally to their FeO content, and (b) their native irons contain a large amount of kamacite, in which the average Ni content is 4–8 wt.%. The same conclusion can be derived for an Apollo 17 anorthositic gabbro, sample 77017. Two Apollo 17 basaltic rocks (70017 and 70215) have the magnetic properties which are similar to those of Apollo 11 mare basalts (Nagata *et al.*, 1970) except

1974LPSC....5.2827N

Table 1. Basic magnetic properties of Apollo 16 and 17 lunar samples.

Magnetic parameter	60016-54 (Br)	61156-11 (Br)	61156-12 (Br)	64435-33 (Br)	70017-73 (Ba)	70017-75 (Ba)	70215-26 (Ba)	74220-41 (F)	75083-13 (F)	77017-40 (AG)Unit	
χ_0(295°K)	2.55	7.63	1.43	—	0.69	0.63	0.33	0.85	12.1	0.44	$\times 10^{-4}$ emu/g/Oe
χ_a(295°K)	0.83	1.72	2.81	0.60	3.9	3.7	3.6	4.0	3.4	1.1	$\times 10^{-5}$ emu/g/Oe
x_a(4.2°K)	12.7	17.1	22.0	8.2	43.7	55.0	50.6	—	50.0	23.9	$\times 10^{-5}$ emu/g/Oe
I_s(295°K)	0.73	1.51	3.80	0.21	0.21	0.22	0.24	0.13	0.22	0.30	emu/g
I_s(4.2°K)	0.99	1.70	4.0	0.24	0.88	0.72	0.89	—	0.90	0.44	emu/g
I_R(295°K)	3.7	3	6	2.9	1.0	1.5	4.4	—	8.5	0.8	$\times 10^{-3}$ emu/g
I_R(4.2°K)	10	15	12	7.5	28.7	33.0	37	—	52	5.0	$\times 10^{-3}$ emu/g
H_c(295°K)	19	7	8	36	7	13	22	—	35	19	Oersteds
H_c(4.2°K)	54	32	13	74	76	136	117	—	160	65	Oersteds
H_{RC}(295°K)	—	450	420	—	70	—	—	—	900	360	Oersteds
Θ	768	771	762	—	782	779	—	778	796	732	°C
Θ*	660	660	683 33	—	None	None	—	None*	None	590	°C
W(Fe)	0.33	0.69	1.74	0.096	0.096	0.10	0.11	0.0060	0.10	0.14	weight %
Ni/(Fe + Ni)	15.0	5.0	4.3 6.0	—	~0	~0	—	~0	~0	7.5	weight %
m_k/m	0.71	0.90	0.96	—	~0	~0	—	~0	~0	0.96	

Remarks: (Br): Breccia, (Ba): Basalt, (F): Fines, (AG): Anorthositic gabbro, W(Fe): Content of metallic iron, m_k/m: Ratio of kamacite component to whole metal, Ni/(Fe + Ni): Ni content in kamacite component.

for considerably small value of the initial magnetic susceptibility (χ_0) of Apollo 17 rocks and a particular ferromagnetic component in the orange soil. The smaller values of χ_0 in Apollo 17 basalts are due to a relatively small amount of superparamagnetically fine grains of native iron. This interpretation can be supported also by a fact that the ratio of viscous magnetization component (ΔI_v) to the stable component (I_0) of isothermal remanent magnetization is considerably small for Apollo 17 samples, as shown in Table 2 (Nagata *et al.* 1973). The orange soil (74220) shows a particular characteristic of its thermomagnetic curve in its initial heating process in about 10^{-5} torr in atmospheric pressure, as illustrated in Fig. 1. In the figure, magnetization (I) shows a maximum peak at about 700°C in the initial heating process, but the peak disappears in the second heating curve, which appears to represent the thermomagnetic curve of an almost pure metallic iron. It seems very likely that a particular ferromagnetic phase of about 700°C in Curie point is in an extremely strong magnetic interaction with an almost pure

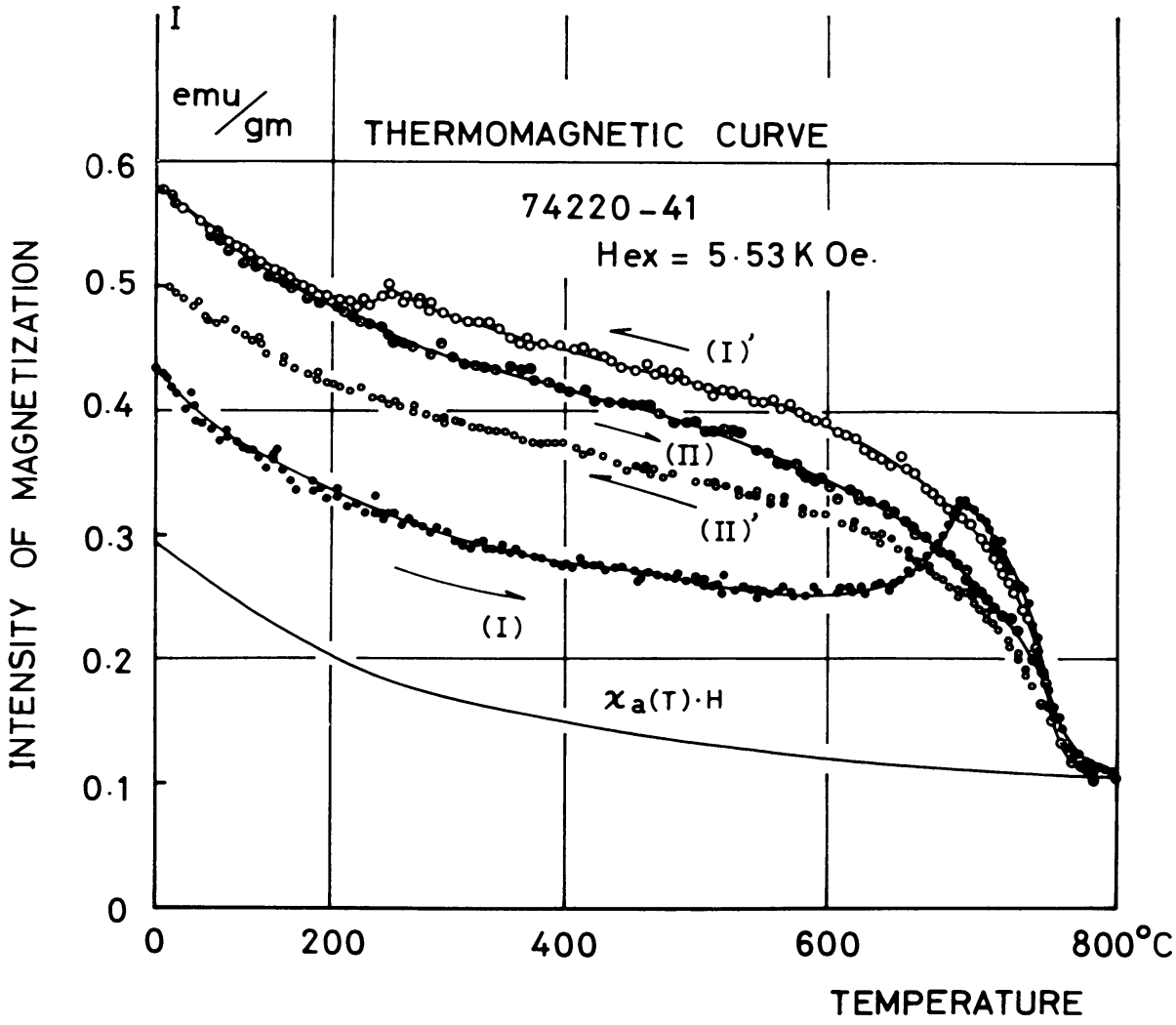

Fig. 1. Thermomagnetic curves of orange soil 74220-41: (I) first run heating, (I)′ first run cooling, (II) second run heating, (II)′ second run cooling.

metallic iron phase in the initial condition, but the particular ferromagnetic phase changes to almost pure metallic iron by heating up to about 800°C. The particular ferromagnetic phase has not yet been exactly identified.

The thermomagnetic curves in the low temperature range (4.2–295°K) show that Apollo 17 basaltic samples such as 70017, 70215, and 75083 contain a considerable amount (about 20 wt.%) of antiferromagnetic ilmenite just as in the case of Apollo 11 mare basaltic materials (Nagata *et al.*, 1970).

Characteristic of Natural Remanent Magnetization

The key parameters to represent characteristics of the natural remanent magnetization (NRM) of Apollo 16 and 17 materials are summarized in Table 2, where (I_n) denotes the specific intensity of NRM after one month storage in nonmagnetic space, (I_0) the relatively stable component of NRM which is defined as the residual magnetization intensity after AF-demagnetizing of 100 Oe · rms, ($\tilde{H}_0$) AF-demagnetizing field to reduce NRM to e^{-1} of the initial value, (h) the intensity of static magnetic field which can produce IRM of the same intensity as I_n, ($\tilde{H}'_0$) AF-demagnetizing field to reduce IRM acquired by h to e^{-1} of the initial value, and $\Delta I_v/I$ the ratio of the viscous magnetization component (ΔI_v) to the stable component (I) of IRM, where I is approximately same as I_n.

As suggested by a comparison of $\tilde{H}_0$ of NRM with $\tilde{H}'_0$ of IRM in Table 2, NRM is much stabler than IRM of the same intensity against the AF-demagnetization. However, none of the eleven lunar samples listed in Table 2 has an extremely stable component of NRM which can remain after the AF-demagnetization of larger than 300 Oe · rms in alternating field and which could be attributed to the thermoremanent magnetization or a remanent magnetization of a similar acquisition mechanism. The categories for the stability of NRM given in the bottom of Table 2 are defined as follows: (1): no significant residual component after 50 Oe · rms AF-demagnetization, (2): no significant residue after 150 Oe · rms demagnetization, and (3): no significant residue after 250 Oe · rms demagnetization. The stable component of NRM of category (3) may have a certain meaning to represent the ancient lunar magnetic field, but it may hardly be attributable to the ordinary thermoremanent magnetization.

Statistics of Magnetic Properties of Apollo Lunar Materials

Figure 2 shows a histogram of Curie point (Θ) of 30 Apollo lunar materials. Curie point values of these Apollo 11–17 samples are distributed between 730°C and 810°C, the dominant median value being 770°C which is in exact agreement of Curie point of pure metallic iron. Curie point of FeNiCo alloys decreases from 770°C with an increase of Ni content, while that of FeNiCo alloys increases from 770°C with an increase of Co. The histogram of (Θ) indicates that Ni content ranges from 0% to 10% and Co content ranges from 0% to about 2% in the lunar materials. Results of analyses of the thermomagnetic curves of these lunar samples can lead to the composition of ferromagnetic metals (e.g. Nagata *et al.*,

Table 2. Characteristics of natural remanent magnetization of Apollo 16 and 17 materials.

Parameter	60016-54 (Br)	61156-11 (Br)	61156-12 (Br)	64435-33 (Br)	70017-73 (Ba)	70017-75 (Ba)	70215-26 (Ba)	73275-15 (Br)	74275-32 (Ba)	77017-40 (AG)	78155-31 (Br)	Unit
I_n	30.0	6.0	12.7	3.9	15.5	20.4	6.6	13.4	4.4	2.8	7.1	$\times 10^{-4}$ emu/g
I_0	1.0	1.1	6.8	0.24	1.9	1.0	1.6	1.1	0.5	0.3	~0	$\times 10^{-6}$ emu/g
$\tilde{H}_0$	12	60	42	20	19	12	21	105	21	9	11	Oe · rms
h	27	6	8	—	6.5	7	12	13	13	5	29	Oersteds
$\tilde{H}'_0$	5	1.5	2	—	5	1.5	2	3	3	1.3	5.5	Oe · rms
$\Delta I_v/I$	1.0	0.91	0.20	—	0.30	0.07	0.07	0.08	0.26	0.12	0.05	
Stability of NRM	(3)	(2)	(3)	(2)	(2)	(2)	(3)	(3)	(2)	(1)	(1)	

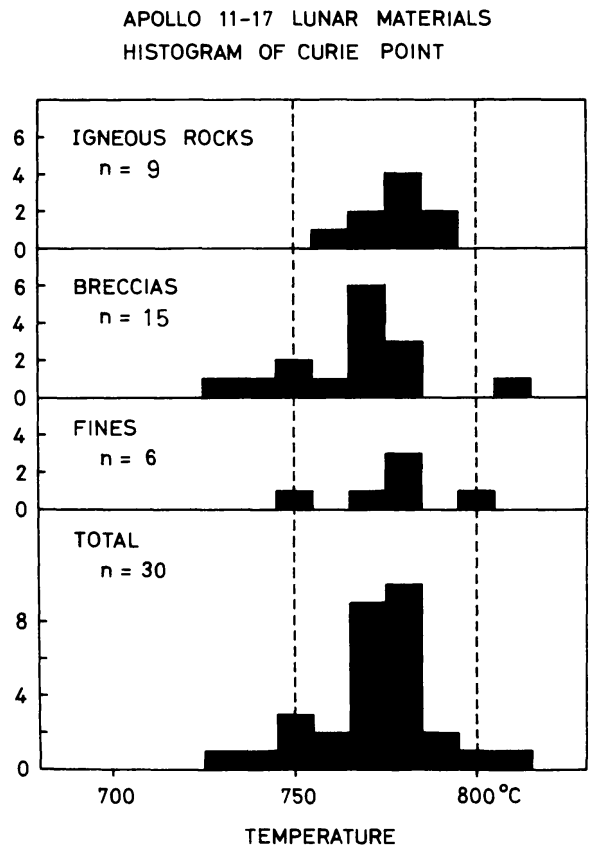

Fig. 2. Histogram of Curie point of Apollo 11–17 lunar materials.

1973). The ferromagnetic metals are either single component of almost pure iron with Co less than 1% or a superposition of the almost pure iron and kamacite of 3–13 wt.% of average Ni content. Figure 3 shows histograms of the ratios of abundance of kamacite component (m_k) to that of the total ferromagnetic metal for 32 Apollo lunar samples. As shown in the figure, the composition of ferromagnetic metals can be classified into two distinct groups, namely a group of almost pure iron with small amounts of Ni and Co ($m_k \simeq 0$) and the other groups containing kamacite component more than a half of the total ferromagnetic metal ($m_k/m \geq 0.5$). Figure 4 illustrates histograms of average Ni contents in the kamacite components in the second group, where the number of the first group (Ni content <1%) also is shown for comparison.

In regard to both histograms of m_k/m and Ni content in kamacite composition, no essential difference can be observed between the group of igneous rocks and the other group of breccias and fines. In histograms of saturation magnetization (I_s) shown in Fig. 5; however, the histogram of I_s of breccias is considerably different from that of igneous rocks. The former has a dominant peak around $I_s = 1$ emu/g (corresponding to about 0.5 wt.% in native iron content), while the latter at $I_s = 0.1$–0.2 emu/g (corresponding to 0.05–0.10 wt.% in native iron content). It seems in the figure that the I_s histogram of lunar fines has both maximum peaks. In the I_s histogram of igneous rocks; however, two exception-

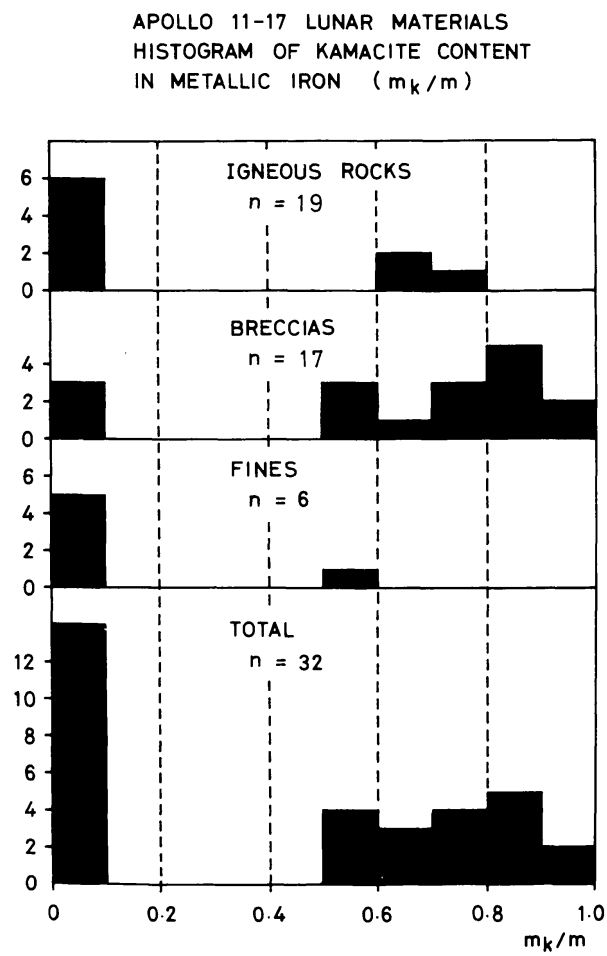

Fig. 3. Histogram of kamacite content in native metal of Apollo 11–17 lunar materials.

ally large values of I_s are observed. They are 14053 (I_s = 2.2 emu/g) and 68415 (I_s = 0.66 emu/g). El Goresy *et al.* (1972) have found that the larger parts of native irons in 14053 are the products of fayalite breakdown. Helz and Appleman (1973) have reported that rock 68415 is very likely to have been produced by impact melting of soils or breccia containing more than one lunar rock type, followed by very rapid cooling. Walker *et al.* (1973) also have concluded that the crystallization of an impact melt of a preexisting cumulate appears to be the most likely mechanism for producing the texture and composition of 68415. If these two samples are eliminated from the group of lunar igneous rocks, I_s values of the other 9 basaltic rocks range only between 0.11 and 0.23 emu/g.

Then, it could be considered that the large values of I_s of lunar breccias and fines are due to either the breakdown of fayalites, ulvöspinels, and ilmenites owing to the meteorite impacts, as postulated by El Goresy *et al.* (1972), or the mixing of meteoritic native metals into the lunar surface materials, as suggested by Goldstein *et al.* (1970, 1971, 1972, 1973) and also by Taylor *et al.* (1973).

Generally speaking, both of the above-mentioned mechanisms can be responsible for the high abundance of native iron in lunar breccias and fines. It must be

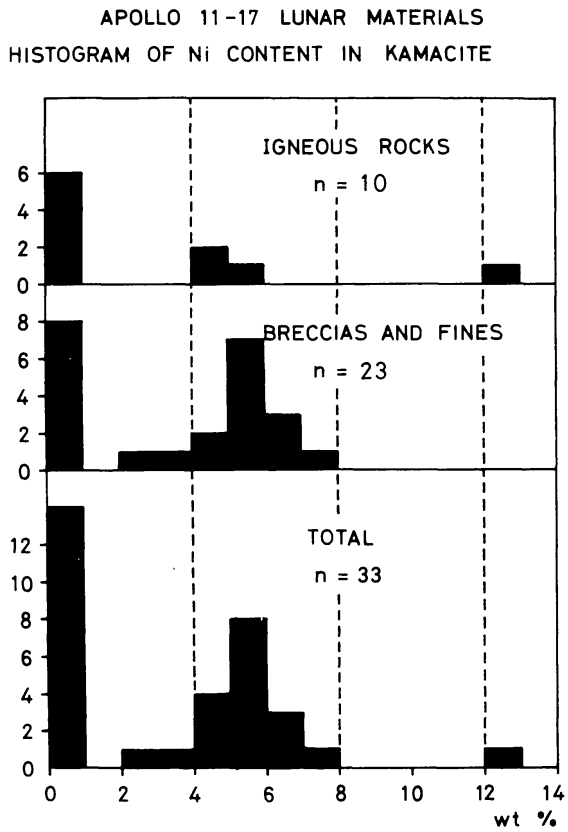

Fig. 4. Histogram of Ni content in kamacite of Apollo 11–17 lunar materials.

emphasized in results of the present study (Fig. 3), however, that all lunar samples whose magnetic properties have been examined to date more or less contain a component of almost pure metallic iron (less than 1 wt.% Ni). In 61156 and 70017, for example, almost all parts of metal are kamacite, but still 4 wt.% of their total metal are almost pure irons. For another example, El Goresy *et al.* (1973) measured contents of Ni and Co in a large number of metal grains in 66095, and found that Ni and Co contents are ranged between 4 and 9 wt.% and between 0.1 and 0.6 wt.%, respectively, which are within Goldstein and Axon's compositional range for meteoritic metal. Results obtained by Taylor *et al.* (1973a) on the same rock also have given the compositional ranges of Ni and Co to be between 4 and 11 wt.% and between 0.15 and 0.6 wt.%, respectively. However, the present magnetic analysis has shown that 82 wt.% of the total metal in 66095 are kamacite of 6 wt.% Ni on average but the remaining 18 wt.% are almost pure iron. Similarly, a microprobe analysis made by Taylor *et al.* (1973b) has shown that the compositional ranges of Ni and Co in metal grains in 60315 are between 4 and 17 wt.% and between 0.25 and 0.35 wt.%, respectively. The present magnetic analysis has shown, on the other hand, that 58 wt.% of the total metal are kamacite of 5 wt.% Ni on average but the remaining 42 wt.% are almost pure iron. It seems most likely that the component of almost pure iron is in form of very fine grains much less than 1 μm in their mean diameter. Actually, experimental data on the viscous magnetization of the lunar samples have clearly indicated that a consider-

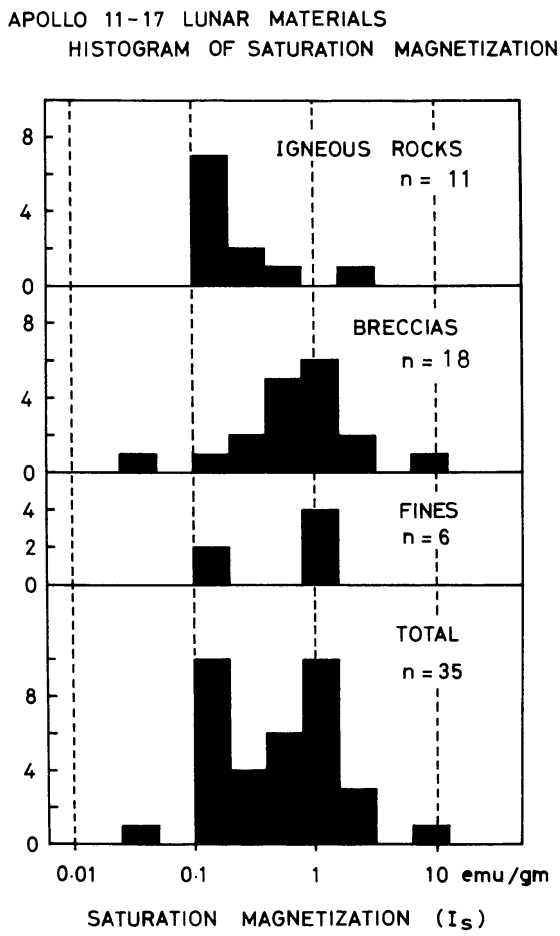

Fig. 5. Histogram of saturation magnetization (I_s) of Apollo 11–17 lunar materials.

able part of ferromagnetic metals are in form of fine grain of 50–300 Å in mean diameter (Nagata *et al.*, 1972, 1973).

The origin of almost pure metallic iron in lunar materials is most likely, at least partly, a product of breakdown of fayalites, ulvöspinels, ilmenites, and other Fe^{2+}-containing minerals as in the case of almost pure metallic iron in 14053. As described by El Goresy *et al.* (1973), for example, 66095 which has a very high I_s value, ($I_s = 9.7$ emu/g), is a highly metamorphosed breccia by meteoritic impacts, and 60315 in which $I_s = 2.6$ emu/g, also is a recrystallized breccia (Hodge and Kushiro, 1973) because of meteoritic impacts. In the case of 60315, Taylor *et al.* (1973b) actually observed evidence of subsolidus reduction of ulvöspinel to ilmenite plus native iron. We may thus be able to conclude that at least a part of almost pure metallic iron in lunar materials is a product of breakdown of Fe-containing opaque minerals caused by severe meteoritic impacts.

Ni Content in Kamacite in Lunar Materials

In the foregoing section, only the average content of Ni in kamacite component in lunar materials is taken into consideration (Fig. 4) except for one case (68415) which contains two distinct kamacite components, 4.5 and 23 wt.% Ni on

average. Since, however, we have the standard thermomagnetic curves to show the $\alpha-\gamma$ transition of stoichiometric FeNi alloys in the cooling process for various values of Ni content, the bulk spectrum of Ni content in kamacite can be obtained by analyzing the thermomagnetic curves of individual lunar samples. Let us express the standard thermomagnetic curve in cooling of FeNi alloy of $\Theta°$ in $\alpha-\gamma$ transition temperature, the observed cooling thermomagnetic curve of a lunar sample, and the spectral density of Θ^0 component by $F(\Theta^0, T)$, $I(T)$, and $n(\Theta^0)$, respectively. Then

$$I(T) = \int n(\Theta^0)F(\Theta^0, T)d\Theta^0 \quad (1)$$

By numerically solving the integral equation given by Eq. (1), we can obtain the density spectrum $n(\Theta^0)$, which can be directly transformed to the density spectrum of Ni content. The density spectra of Ni, n(Ni), thus obtained for individual lunar samples are in fairly good agreement with those obtained by microprobe analysis of a large number of metallic grains of the same samples. For example, the magnetically obtained spectrum, n(Ni), of 66095 is mostly extended between 4 and 10 wt.% Ni and has a sharp maximum in a range of 5–7 wt.% Ni, which is in good agreement with the results of analyses made by El Goresy *et al.* (1973) and Taylor *et al.* (1973b). The magnetically obtained n(Ni) of 68415 has a broad and flat distribution between 3 and 27 wt.% Ni having small maxima around 5 and 14 wt.% Ni, which is in good agreement with the result obtained by Taylor *et al.* (1973).

Figure 6 illustrates the average spectra of n(Ni) for 3 igneous rocks and 12 breccias and fines, in which kamacite is the major component of native metal, together with three examples of similar spectrum of carbonaceous and ordinary chondrites for comparison. It will be clearly observed in the figure that n(Ni) spectra of lunar igneous rocks and breccias and fines are very similar to each other, having a maximum peak around 6.5 wt.% Ni and extending nearly to 30 wt.% Ni, and that both n(Ni) spectra have another peak at zero Ni content. (The minus values of Ni content in Fig. 6 represents the effect of Co, namely Ni $\simeq$ 0 and Co = finite.)

On the contrary, three n(Ni) spectra of meteorite have a sharp lower limit cut at about 3.5 wt.% Ni, though they also have a maximum peak around 5–6 wt.% Ni. It may be further observed that n(Ni) spectrum of lunar materials is more similar to that of carbonaceous chondrite than that of ordinary chondrite which has a sharp upper limit cut at about 7 wt.% Ni.

It will be again stated, therefore, that the native metal in lunar materials contains an almost pure iron component, which is not contained in meteorites. As far as data shown in Fig. 6 are concerned, it will be further noted that the cooling condition of lunar rocks appears to be somewhat similar to that of carbonaceous chondrites.

Summary

All lunar materials whose magnetic properties have been examined to date more or less contain a metallic component of almost pure iron composition. On the other hand, most lunar breccias and fines contain native iron (or native FeNi)

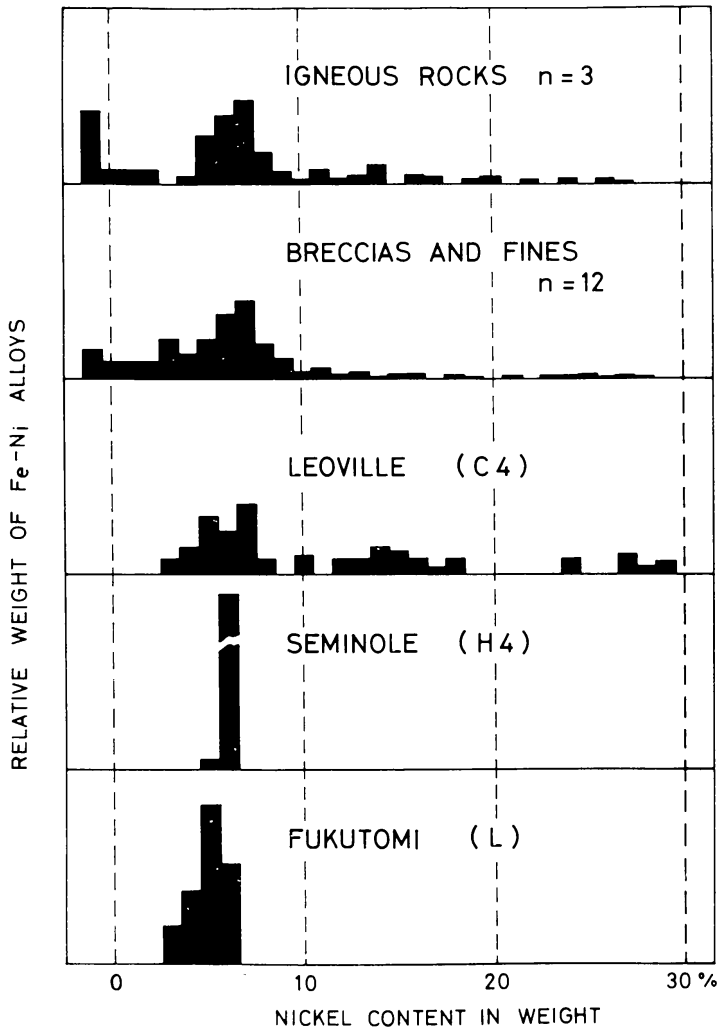

Fig. 6. Ni content spectra in lunar igneous rocks, breccias, fines and three meteorites.

about ten times as much as that in lunar basaltic rocks which have not been seriously shock metamorphosed. In particular, a highly shock metamorphosed rock 60315 contains 1.9 wt.% of almost pure iron in addition to 2.6 wt.% of kamacite of 5 wt.% in average Ni content. Since meteoritic native metals do not contain the almost pure iron component, the observed high abundance of almost pure iron in lunar breccias and fines is almost likely to be due to the product of breakdown of fayalites, ulvöspinel, ilmenite, and others caused by severe meteoritic impacts, as observed by El Goresy *et al.* for 14053 which contains about 1.0 wt.% of almost pure iron. As the abundance of kamacite component also is high in lunar breccias and the composition of lunar kamacite is not so much different from that of meteoritic kamacite, it also may be true that the high abundance of kamacite in lunar breccias and some fines is due to the mixing of meteoritic metal into the lunar surface materials.

References

El Goresy A., Taylor L. A., and Ramdohr P. (1972) Fra Mauro crystalline rocks: Mineralogy, geochemistry and subsolidus reduction of the opaque minerals. *Proc. Third Lunar Sci. Conf., Geochim. Cosmochim. Acta*, Suppl. 3, Vol. 1, pp. 333–349. MIT Press.

El Goresy A., Ramdohr P., and Medenbach O. (1973) Lunar samples from Descartes site: Opaque mineralogy and geochemistry. *Proc. Fourth Lunar Sci. Conf., Geochim. Cosmochim. Acta*, Suppl. 4, Vol. 1, pp. 733–750. Pergamon.

Goldstein J. I. and Axon H. J. (1973) Composition, structure, and thermal history of metallic particles from 3 Apollo 16 soils, 65701, 68501 and 63501. *Proc. Fourth Lunar Sci. Conf., Geochim. Cosmochim. Acta*, Suppl. 4, Vol. 1, pp. 751–775. Pergamon.

Goldstein J. I. and Yakowitz H. (1971) Metallic inclusion and metal particles in the Apollo 12 lunar soil. *Proc. Second Lunar Sci. Conf., Geochim. Cosmochim. Acta*, Suppl. 2, Vol. 1, pp. 177–191. MIT Press.

Goldstein J. I., Henderson E. P., and Yakowitz H. (1970) Investigation of Lunar metal particles. *Proc. Apollo 11 Lunar Sci. Conf., Geochim. Cosmochim. Acta*, Suppl. 1, Vol. 1, pp. 499–512. Pergamon.

Goldstein J. I., Axon H. J., and Yen C. F. (1972) Metallic particles in the Apollo 14 lunar soil. *Proc. Third Lunar Sci. Conf., Geochim. Cosmochim. Acta*, Suppl. 3, Vol. 1, pp. 1037–1064. MIT Press.

Helz R. T. and Appleman D. E. (1973) Mineralogy, petrology and crystallization history of Apollo 16 rock 68415. *Proc. Fourth Lunar Sci. Conf., Geochim. Cosmochim. Acta*, Suppl. 4, Vol. 1, pp. 643–659. Pergamon.

Hodge F. N. and Kushiro I. (1973) Petrology of Apollo 16 lunar high land rocks. *Proc. Fourth Lunar Sci. Conf., Geochim. Cosmochim. Acta*, Suppl. 4, Vol. 1, pp. 1033–1048. Pergamon.

Nagata T., Ishikawa Y., Kinoshita H., Kono M., Syono Y., and Fisher R. M. (1970) Magnetic properties and natural remanent magnetization of Apollo 11 lunar materials. *Proc. Apollo 11 Lunar Sci. Conf., Geochim. Cosmochim. Acta*, Suppl. 1, Vol. 3, pp. 2325–2340. Pergamon.

Nagata T., Fisher R. M., Schwerer F. C., Fuller M. D., and Dunn J. R. (1971) Magnetic properties and remanent magnetization of Apollo 12 lunar materials in Apollo 11 lunar microbreccia. *Proc. Second Lunar Sci. Conf., Geochim. Cosmochim. Acta*, Suppl. 2, Vol. 3, pp. 2461–2476. MIT Press.

Nagata T., Fisher R. M., and Schwerer F. C. (1972a) Lunar rock magnetism. *The Moon* **4**, 160–186.

Nagata T., Fisher R. M., Schwerer F. C., Fuller M. D., and Dunn J. R. (1972b) Rock magnetism of Apollo 14 and 15 materials. *Proc. Third Lunar Sci. Conf., Geochim. Cosmochim. Acta*, Suppl. 3, Vol. 3, pp. 2423–2447. MIT Press.

Nagata T., Fisher R. M., Schwerer F. C., Fuller M. D., and Dunn J. R. (1973) Magnetic properties and natural remanent magnetization of Apollo 15 and 16 lunar materials. *Proc. Fourth Lunar Sci. Conf., Geochim. Cosmochim. Acta*, Suppl. 4, Vol. 3, pp. 3019–3043. Pergamon.

Taylor L. A., McCallister R. H., and Sardi O. (1973a) Cooling histories of lunar rocks based on opaque mineral geothermometries. *Proc. Fourth Lunar Sci. Conf., Geochim. Cosmochim. Acta*, Suppl. 4, Vol. 1, pp. 819–828. Pergamon.

Taylor L. A., Mao H. K., and Bell P. M. (1973b) "Rust" in the Apollo 16 rocks. *Proc. Fourth Lunar Sci. Conf., Geochim. Cosmochim. Acta*, Suppl. 4, Vol. 1, pp. 829–839. Pergamon.

Walker D., Longhi J., Grove T. L., Stolper E., and Hays J. F. (1973) Experimental petrology and origin of rocks from the Descartes highlands. *Proc. Fourth Lunar Sci. Conf., Geochim. Cosmochim. Acta*, Suppl. 4, Vol. 1, pp. 1013–1032. Pergamon.